CORRECTED 15 APRIL 2011; SEE LAST PAGE

Selective inhibition of the cyclic guanosine monophosphate (cGMP)–dependent kinase PfPKG with 4-[2-(fluorphenyl)-5-(1-methylpiperidine-4-yl)-1*H* pyrrol-3-yl]pyridine (compound 1) blocks egress (*21*). Treatment of schizonts with compound 1 inhibited processing of PfMSP1 by PfSUB1 (fig. S6A). However, compound 1 did not inhibit PfSUB1 enzyme activity directly (fig. S6B), suggesting that compound 1 treatment interferes with access of PfSUB1 to its endogenous substrates, perhaps by preventing exoneme discharge.

To determine whether PfCDPK5-deficient merozoites are capable of erythrocyte invasion, we mechanically disrupted arrested schizonts by needle-shearing. Newly invaded rings were observed at a significantly higher rate in the sheared cultures compared with unsheared controls (Fig. 3B). Thus, the egress trigger may be distinct from the erythrocyte invasion trigger. Isolation of viable PfCDPK5-deficient merozoites provides a valuable source for studies of erythrocyte invasion. In contrast to the invasion-competent PfCDPK5-deficient merozoites, mechanically disrupted compound 1–treated parasites did not generate newly invaded rings (Fig. 3B), consistent with these parasites being blocked at an earlier step.

We propose a modified model of *P. falciparum* egress from erythrocytes (fig. S7). The protease cascade is necessary but not sufficient for parasite egress. After an egress trigger, a transient increase in Ca^{2+} concentration activates PfCDPK5 to amplify and transmit the signal for parasite egress. The final stages of PVM and erythrocyte PM rupture probably involve molecules downstream of PfCDPK5 activation, such as perforin-like proteins, membrane channels, and/or proteases (*22*, *23*).

References and Notes

1. O. Billker *et al.*, *Cell* **117**, 503 (2004).
2. A. Coppi *et al.*, *Cell Host Microbe* **2**, 316 (2007).
3. P. M. Färber, R. Graeser, R. M. Franklin, B. Kappes, *Mol. Biochem. Parasitol.* **87**, 211 (1997).
4. J. L. Green *et al.*, *J. Biol. Chem.* **283**, 30980 (2008).
5. T. Ishino, Y. Orito, Y. Chinzei, M. Yuda, *Mol. Microbiol.* **59**, 1175 (2006).
6. N. Kato *et al.*, *Nat. Chem. Biol.* **4**, 347 (2008).
7. H. Kieschnick, T. Wakefield, C. A. Narducci, C. Beckers, *J. Biol. Chem.* **276**, 12369 (2001).
8. Y. Zhao, B. Kappes, R. M. Franklin, *J. Biol. Chem.* **268**, 4347 (1993).
9. K. G. Le Roch *et al.*, *Science* **301**, 1503 (2003).
10. J. F. Harper, A. Harmon, *Nat. Rev. Mol. Cell Biol.* **6**, 555 (2005).
11. Materials and methods are available as supporting material on *Science* Online.
12. C. M. Armstrong, D. E. Goldberg, *Nat. Methods* **4**, 1007 (2007).
13. L. A. Banaszynski, L.-C. Chen, L. A. Maynard-Smith, A. G. L. Ooi, T. J. Wandless, *Cell* **126**, 995 (2006).
14. A. Herm-Götz *et al.*, *Nat. Methods* **4**, 1003 (2007).
15. I. Russo, A. Oksman, B. Vaupel, D. E. Goldberg, *Proc. Natl. Acad. Sci. U.S.A.* **106**, 1554 (2009).
16. B. W. Chu, L. A. Banaszynski, L.-C. Chen, T. J. Wandless, *Bioorg. Med. Chem. Lett.* **18**, 5941 (2008).
17. C. Möskes *et al.*, *Mol. Microbiol.* **54**, 676 (2004).
18. S. Arastu-Kapur *et al.*, *Nat. Chem. Biol.* **4**, 203 (2008).
19. S. Yeoh *et al.*, *Cell* **131**, 1072 (2007).
20. K. Koussis *et al.*, *EMBO J.* **28**, 725 (2009).
21. H. M. Taylor *et al.*, *Eukaryot. Cell* **9**, 37 (2010).
22. R. Chandramohanadas *et al.*, *Science* **324**, 794 (2009).
23. B. F. Kafsack *et al.*, *Science* **323**, 530 (2009).

24. We thank K. Kettleborough, S. Osborne, and colleagues at Medical Research Council (MRC) Technology for provision of compound 1, S. Badrinath, E. Duraisingh, C. Merrick, and B. Coleman for critical reading of the manuscript, and D. Wirth for essential guidance and support. This work was supported by Pediatric Scientist Development Program Fellowship awards K12-HD000850 (J.D.D. and S.D.P.), National Institutes of Health R01 grant R01AI057919 (M.T.D.), a Burroughs Wellcome Fund New Investigator in the Pathogenesis of Infectious Diseases Fellowship (M.T.D.), the MRC UK U117532063 (M.J.B.), a Wellcome Trust Project grant 086550 (C.R.C.), the NIH GM073046 (T.J.W.), and an EU FP7 grant MALSIG 223044 (D.A.B.).

Supporting Online Material

www.sciencemag.org/cgi/content/full/328/5980/910/DC1
Materials and Methods
SOM Text
Figs. S1 to S7
References
Data File S1

10 February 2010; accepted 13 April 2010
10.1126/science.1188191

Small RNA Duplexes Function as Mobile Silencing Signals Between Plant Cells

Patrice Dunoyer,[1]* Gregory Schott,[1] Christophe Himber,[1] Denise Meyer,[1] Atsushi Takeda,[2] James C. Carrington,[2] Olivier Voinnet[1]*

In the plant RNA interference (RNAi) pathway, 21-nucleotide duplexes of small interfering RNA (siRNA) are processed from longer double-stranded RNA precursors by the RNaseIII Dicer-like 4 (DCL4). Single-stranded siRNAs then guide Argonaute 1 (AGO1) to execute posttranscriptional silencing of complementary target RNAs. RNAi is not cell-autonomous in higher plants, but the nature of the mobile nucleic acid(s) signal remains unknown. Using cell-specific rescue of DCL4 function and cell-specific inhibition of RNAi movement, we genetically establish that exogenous and endogenous siRNAs, as opposed to their precursor molecules, act as mobile silencing signals between plant cells. We further demonstrate physical movement of mechanically delivered, labeled siRNA duplexes that functionally recapitulate transgenic RNAi spread. Cell-to-cell movement is unlikely to involve AGO1-bound siRNA single strands, but instead likely involves siRNA duplexes.

In plants, RNAi spreads over long distances through the vasculature and from cell to cell presumably via plasmodesmata, owing to mobile nucleic acid–based signals (*1*, *2*). Plant cell-to-cell RNAi movement has defensive and developmental roles: The spread of viral-derived silencing signals probably immunizes surrounding naïve cells (*3*), whereas movement of silencing signals from endogenous *TRANS-ACTING siRNA* (*TAS*) (siRNA, small interfering RNA) loci might generate target gene–expression gradients allowing organ polarization (*4*, *5*). Movement of small RNA is also suspected to account for epigenetic reprogramming between pollen nuclei (*6*). Both viruses and *TAS* loci produce long double-stranded RNA (dsRNA) precursors, subsequently converted into siRNAs by Dicer-like 4 (DCL4), one of four *Arabidopsis* Dicer-like proteins (*3*, *7*). Although DCL4-dependent siRNAs are popular candidates as cell-to-cell RNAi signaling molecules (*5*, *8*), a role for their precursors, including long dsRNA, cannot be excluded. Consequently, the nature of the mobile, silencing nucleic acid(s) remains unknown (*9*).

In the experimental SUC:*SUL Arabidopsis* system, a long-dsRNA–producing transgene is expressed under the phloem-companion cell-specific promoter, SUC2 (*8*). This triggers non–cell-autonomous RNAi of the ubiquitously expressed endogenous *SULFUR* (*SUL*) mRNA, generating a leaf chlorotic phenotype that expands 10 to 15 cells beyond the vasculature (Fig. 1A). The *SUL* dsRNA is processed into DCL4-dependent 21-nucleotide (nt) and DCL3-dependent 24-nt siRNAs, which are, respectively, mandatory and dispensable for the manifestation of *SUL*-silencing movement (Fig. 1B) (*8*). To uncover the *SUL*-silencing signal's identity we used the viral silencing suppressor P19, which specifically sequesters 21–base pair (bp) siRNA duplexes, but not their long-dsRNA precursor (*10*). A SUC:*P19* transgene was introduced into SUC:*SUL* plants. Highly expressing lines displayed no *SUL*-silencing movement, whereas movement remained unaltered in low-expressing lines (Fig. 1A). As expected, both high and low P19 lines accumulated similar amounts of each *SUL* siRNA species, as found in SUC:*SUL* reference plants (Fig. 1, A and B). Immunoprecipitation analyses using transgenic lines expressing different levels of epitope-tagged P19 (SUC:*P19HA*) revealed that *SUL*-silencing suppression was

[1]Institut de Biologie Moléculaire des Plantes du CNRS, Université de Strasbourg 12 rue du Général Zimmer, 67084 Strasbourg cedex, France. [2]Center for Genome Research and Biocomputing, Oregon State University, Corvallis, OR 97331, USA.

*To whom correspondence should be addressed. E-mail: patrice.dunoyer@ibmp-ulp.u-strasbg.fr (P.D.); olivier.voinnet@ibmp-ulp.u-strasbg.fr (O.V.)

correlated with the extent to which 21-nt *SUL* siRNAs were sequestered by P19 (Fig. 1, C to E). Immunostaining in SUC:*P19HA* plants and immunofluorescence analyses carried out in independently generated SUC:*SUL2*/SUC:*P19HA* lines confirmed that P19HA accumulation is strictly confined within phloem-companion cells (Fig. 1F and fig. S1). The strict cell autonomy of P19 was further confirmed by analysis of independent transgenics in which the protein was driven under a mesophyll-specific promoter (fig. S1). We conclude that suppression of cell-to-cell *SUL*-silencing movement relies on the dose-dependent and cell-autonomous capacity of P19 to specifically sequester DCL4-dependent 21-bp *SUL* siRNAs in silencing-incipient cells. Similar conclusions were drawn using SUC:*SUL* plants expressing companion-cell–specific P21, a distinct silencing suppressor that, like P19, sequesters 21-nt siRNA (fig. S2) (*11*).

As a second approach to unravel the signal's identity, we investigated cell-type–specific requirements for DCL4 in the *SUL*-silencing movement process. A requirement for DCL4 in incipient, dsRNA-producing companion-cells, but not in recipient cells, would support movement of an siRNA signal (*9*). A *DCL4* genomic fragment was cloned under the *SUC2* promoter (SUC:*DCL4*) and transformed into SUC:*SUL* plants carrying a *dcl4-2* null mutation. Without a DCL4 transgene, *dcl4-2* plants lack 21-nt *SUL* siRNAs and, accordingly, display no *SUL*-silencing movement (Fig. 2, A and B). Lack of *DCL4* results in aberrant processing of endogenous *TAS* precursors into nonfunctional, 22-nt-long siRNAs by DCL2 (Fig. 2B). Consequently, leaves ectopically accumulate high levels of trans-acting siRNA (tasiRNA) targets, including *AUXIN RESPONSE FACTOR 3* (*ARF3*) transcripts, which normally undergo TAS3 tasiRNA-dependent non–cell-autonomous RNAi over several leaf-primordia cell layers (Fig. 2C) (*4*, *5*). DCL4 expression was detected in nearly all independently generated SUC:*DCL4*/SUC:*SUL*/*dcl4* transgenic lines (fig. S3), and in those lines, 21-nt *SUL* siRNA accumulation was fully rescued (Fig. 2B). Companion-cell–restricted DCL4 expression also rescued full *SUL*-silencing movement (Fig. 2A). This result suggests that movement of *SUL* long dsRNA, if any, cannot account for the SUL-silencing phenotype. Furthermore, 21-nt-long tasiRNA production was also restored in leaves, as was down-regulation of *ARF3* and other endogenous tasiRNA targets (Fig. 2, B and C). Consistent with this finding, leaf expression of Argonaute 7 (AGO7), a limiting factor in the *TAS3* pathway, is restricted to the vasculature and cells near the abaxial surface (*12*). Collectively, these data indicate that 21-nt siRNAs account for cell-to-cell movement of exogenous, and possibly endogenous, DCL4-dependent RNAi.

SUL-silencing requires the specific loading of 21-nt *SUL* siRNA guide strands into AGO1 (*8*), 1 of 10 *Arabidopsis* AGO proteins that also effects posttranscriptional silencing with endogenous microRNAs (miRNAs) and tasiRNAs (*13*). Therefore, we investigated whether 21-nt siRNAs move between cells in association with AGO1. AGO1 immunoprecipitation experiments conducted in independent SUC:*SUL* lines expressing the SUC:*P19HA* or SUC:*P19* transgenes showed that approximately half of the 21-nt *SUL* siRNA pool is sequestered away from AGO1 by phloem-specific P19 (Fig. 3A); this sequestration is sufficient to prevent *SUL*-silencing movement (Fig. 1, A and C). Similar observations were made in SUC:*SUL* plants expressing SUC:*P21* or SUC:*P21HA* (fig. S2). As the other half of the companion-cell–derived 21-nt *SUL* siRNA remains loaded

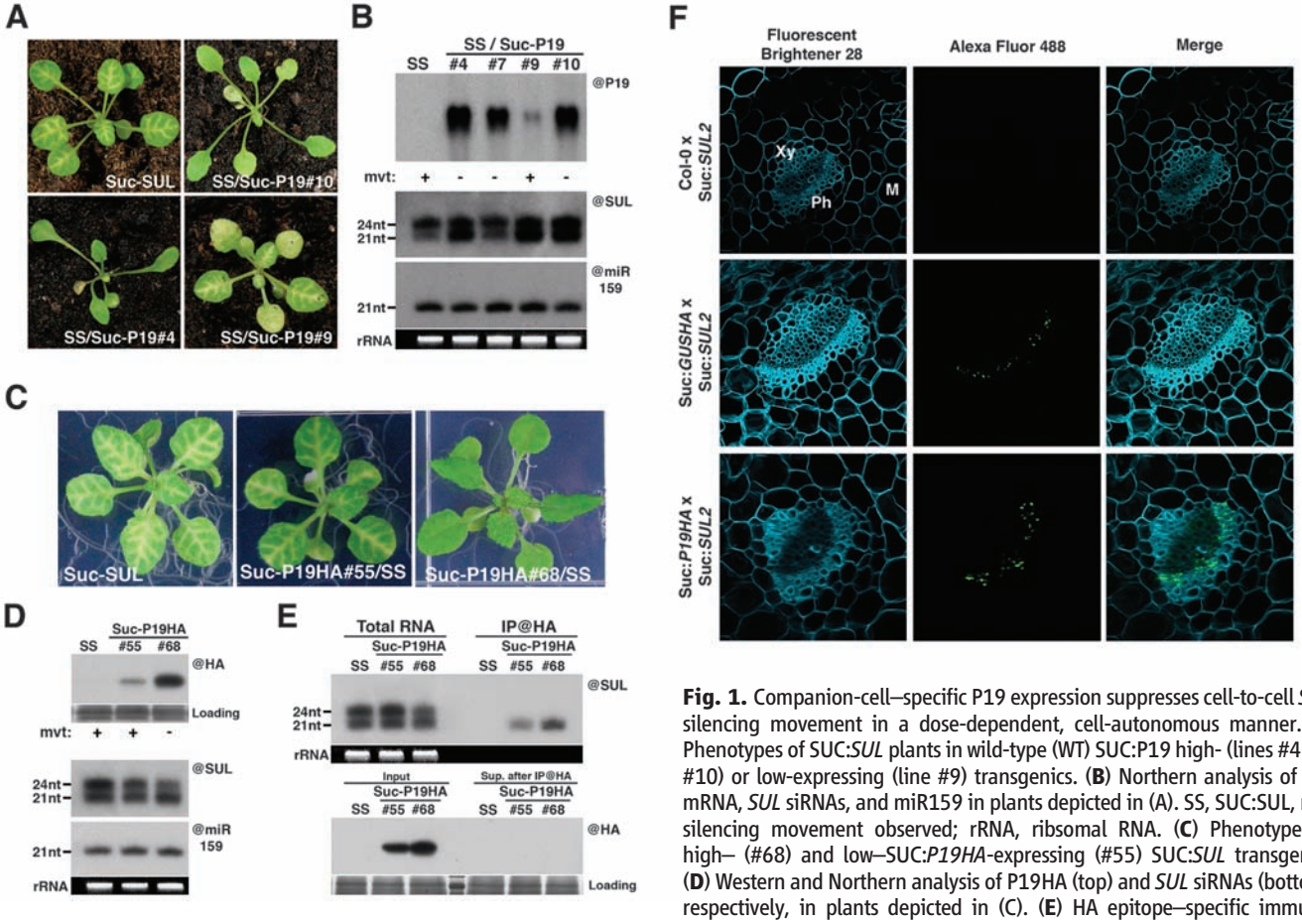

Fig. 1. Companion-cell–specific P19 expression suppresses cell-to-cell *SUL*-silencing movement in a dose-dependent, cell-autonomous manner. (**A**) Phenotypes of SUC:*SUL* plants in wild-type (WT) SUC:P19 high- (lines #4 and #10) or low-expressing (line #9) transgenics. (**B**) Northern analysis of *P19* mRNA, *SUL* siRNAs, and miR159 in plants depicted in (A). SS, SUC:SUL, mvt, silencing movement observed; rRNA, ribsomal RNA. (**C**) Phenotypes of high– (#68) and low–SUC:*P19HA*-expressing (#55) SUC:*SUL* transgenics. (**D**) Western and Northern analysis of P19HA (top) and *SUL* siRNAs (bottom), respectively, in plants depicted in (C). (**E**) HA epitope–specific immunoprecipitation in SUC:*SUL* reference plants or in high– and low–SUC:*P19HA*-expressing SUC:*SUL* transgenics. Total RNA was extracted from immunoprecipitates (IPs), and low–molecular-weight RNA was subjected to Northern analysis (top). P19HA immunoprecipitation was confirmed by protein blot analysis (bottom). (**F**) P19HA immunolocalization (Alexa-Fluor488) in transverse sections of SUC:*P19HA*-expressing SUC:*SUL* transgenics. Plants expressing a SUC:*GUSHA* transgene provide a positive control for companion-cell immunolabeling retention. Cell walls were stained with fluorescent brightener 28. Xy, Xylem; Ph, Phloem; M, Mesophyll.

into AGO1 (Fig. 3A), it is unlikely that siRNAs move from cell to cell in an AGO1-bound form. Furthermore, AGO1-bound siRNA movement would entail movement of AGO1 itself. To address this issue, a SUC2-driven, functional epitope-tagged *AGO1* allele (SUC:*FLAG-AGO1*) (*14*) was transformed into SUC:*SUL* plants carrying either the *ago1-12* or *ago1-27* hypomorphic mutations, both of which prevent *SUL*-silencing movement with minimal or no effect on *SUL* siRNA production (Fig. 3, B and D, and fig. S4) (*8*, *15*). Of the five lines inspected, none recovered the *SUL*-silencing movement phenotype (Fig. 3B and fig. S4), despite FLAG-AGO1 being appropriately loaded with the 21-nt *SUL* siRNAs and with endogenous miRNAs (Fig. 3, C and D, and fig. S4). We conclude that AGO1 is required cell-autonomously for the execution of RNAi in incipient and recipient cells. Therefore, DCL4-dependent siRNAs are unlikely to move between cells bound to AGO1.

Next, we performed experiments to directly monitor siRNA movement in plants. We used particle bombardment to mechanically deliver various RNAi trigger molecules into XD216 transgenic seedlings. XD216 contains a constitutively expressed *GREEN FLUORESCENT PROTEIN* (*GFP*) transgene in an *sde1/rdr6* null mutant background (*16*). This mutation ensures that any silencing events monitored in XD216 are attributable to the bombarded material, as opposed to endogenously amplified and RDR6-dependent secondary silencing events (fig. S5) (*16*). Bombardment of in vitro transcribed and preannealed *GFP*-derived dsRNA consistently triggered *GFP* silencing: Four days post-bombardment (dpb), it was manifested as foci, 10 to 15 cells in diameter, that did not expand any further (Fig. 4A). The same observation was made by bombarding a mix of three chemically synthesized, 21-bp *GFP* siRNA duplexes (Fig. 4B), but not by bombarding siRNAs or dsRNA with *GFP*-unrelated sequences. Bombarding particles co-coated with a GUS-reporter gene plasmid confirmed that silencing foci resulted from bona fide *GFP*-silencing movement radiating from primarily delivered, individual cells or small groups of cells (Fig. 4, C and D). The GFP-silencing–

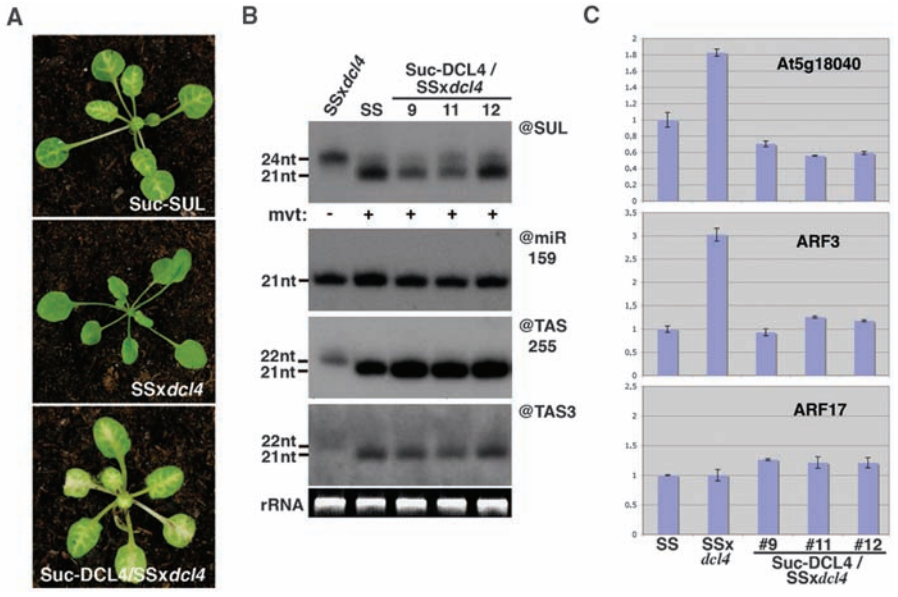

Fig. 2. Companion-cell–specific *DCL4* expression in SUC:*SUL*/*dcl4* mutants restores 21-nt *SUL* siRNA and tasiRNA accumulation, cell-to-cell *SUL*-silencing movement, and tasiRNA target down-regulation. (**A**) *SUL*-silencing phenotype in WT, *dcl4*, and SUC:*DCL4*/*dcl4* transgenic plants. (**B**) Northern analysis of *SUL* siRNAs, miR159, TAS1 siRNA255, and TAS3 tasiRNAs in WT, *dcl4*, and independent SUC:*DCL4*/*dcl4* transgenics (#9, #11, #12). (**C**) Quantitative reverse transcription polymerase chain reaction analysis of endogenous *TAS1 siRNA255* (*At5g18040*) and *TAS3* tasiRNA (*ARF3*) target mRNA accumulation. *ARF17* mRNA (miR160 target) was used as a nonaffected control. cDNA inputs were normalized to Actin2 mRNA; expression ratios are relative to levels in the SUC:*SUL* parental line. Data are displayed as averages ± SD (indicated by error bars) (three replicates).

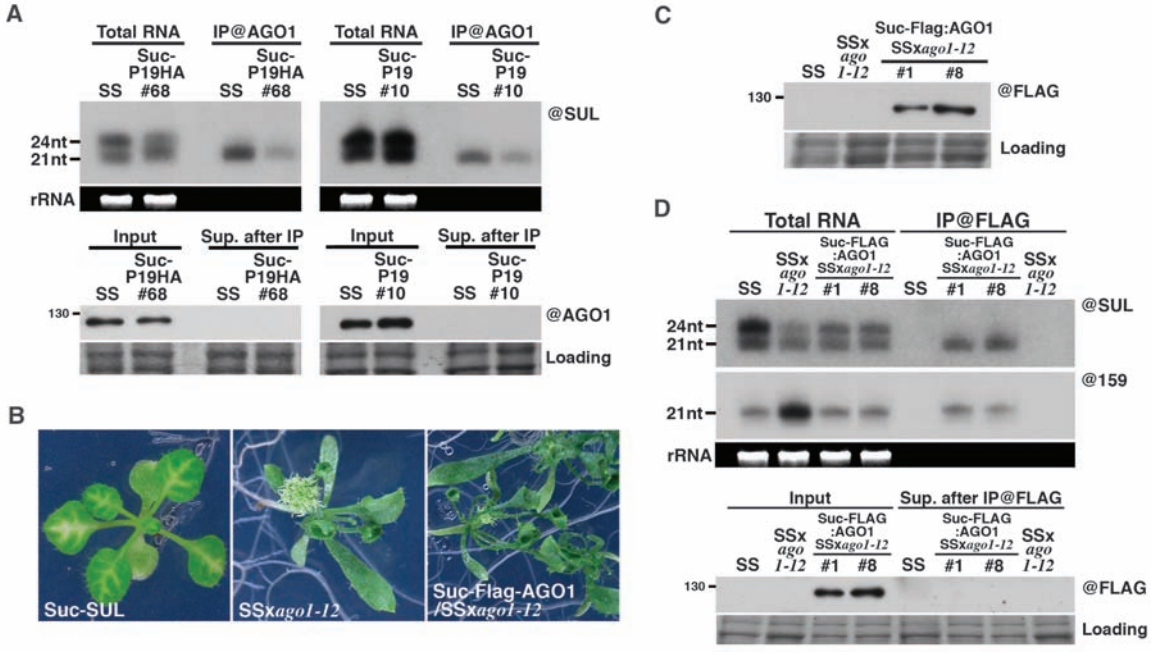

Fig. 3. Cell-autonomous requirement for AGO1 in *SUL* silencing. (**A**) Northern analysis of total RNA and IP fractions of AGO1-bound small RNA in control, SUC:*P19*-, or SUC:*P19HA*-expressing SUC:*SUL* plants (top). AGO1 immunoprecipitation was confirmed by protein blot analysis (bottom). (**B**) *SUL*-silencing in SUC:*SUL* WT, *ago1-12*, and SUC:*FLAG-AGO1*/*ago1-12* trangenic plants. (**C**) Western analysis of FLAG-AGO1 in two independent SUC:*FLAG-AGO1*/*ago1-12* transgenic lines. (**D**) FLAG-specific immunoprecipitation in SUC:*SUL* WT, *ago1-12*, and SUC:*FLAG-AGO1*/*ago1-12* transgenic plants and Northern analysis of *SUL* siRNA and miR159 accumulation in total RNA or FLAG-AGO1 IP (top). Protein blot analysis confirmed FLAG-AGO1 immunoprecipitation (bottom).

movement process was recapitulated upon bombardment of individual siRNA duplexes (Fig. 4, E and F), but not with single-stranded guide or passenger strands (fig. S5). Moreover, those chemically synthesized siRNA duplexes were faithfully and functionally sorted into cognate AGO effector complexes in bombarded and, presumably, surrounding cells (fig. S5).

To test if *GFP*-silencing foci in XD216 resulted from direct cell-to-cell movement of the bombarded siRNAs, the passenger-stand in the siRNA 6768 duplex was covalently labeled at its 3′ end with the fluorophore ALEXA555 (*17*). One hour pb (hpb), the fluorescence was typically concentrated in single cells, or small groups of cells (Fig. 4G), but by 4 hpb, it had radiated from the initially delivered area into the surrounding cells, a pattern unchanged at 20 hpb and beyond (Fig. 4, H to K). This pattern was unlikely to result from movement of free fluorophore or partially digested siRNAs, as the residual fluorescence was precisely superimposed over *GFP*-silencing foci in many areas of bombarded leaves at 4 dpb (Fig. 4, L and M, and fig. S5). The most straightforward interpretation of these results is that labeled siRNA 6768 had moved from the bombarded cells to the adjacent 10 to 15 cells and triggered RNAi. Bombarding the siRNA 6768 duplex with a 3′ end–labeled guide strand also triggered movement, but *GFP*-silencing efficacy was reduced, presumably because the ALEXA555 dye prevents optimal loading of guide strands into AGOs. Occasionally, labeled siRNAs reached the vascular system during the cell-to-cell movement process (Fig. 4, N to P). Moreover, singly bombarded phloem cells could clearly transmit siRNAs to adjacent cells within vascular bundles (Fig. 4, Q and R), suggesting that siRNAs may also act as phloem-transported signals for long-distance silencing in *Arabidopsis* (*18*, *19*).

We have provided genetic evidence that siRNAs are necessary for mobile silencing, while the bombardment experiments show that they are also sufficient for this process. We conclude, therefore, that siRNAs act as silencing signals between plant cells and, possibly, over long distances (*19*). Although their exact mobile form (that is, protein-bound versus free molecules) awaits further characterization, duplexes, as opposed to single strands, are likely involved. Indeed, movement occurred with preannealed siRNA duplexes containing either a labeled passenger strand or a labeled guide strand. The former is rapidly turned over upon strand separation (*20*), whereas guide single strands are usually unstable unless loaded into AGOs (*21*); yet AGO1, the effector of mobile RNAi, functions cell-autonomously (Fig. 3, B to D). Lack of *GFP*-silencing foci upon bombardment of anti-*GFP* single strands also supports movement of siRNAs as duplexes (fig. S5), although single strands might be rapidly degraded in bombarded cells or might fail to incorporate into AGO1 in surrounding cells owing to prerequisite strand separation. Movement of 21-bp siRNA duplexes between cells and their inhibition by viral P19 agree with previous results obtained with the P19-producing *Cymbidium ringspot virus* (CymRSV): P19 was dispensable for CymRSV accumulation within vascular bundles. However, its lack prevented further invasion of the leaf lamina, which, although virus-free, exhibited nucleotide sequence-specific resistance to CymRSV owing to the onset and cell-to-cell movement of a mobile, virus-induced silencing signal (*22*). In light of the present results, this signal must be the DCL4-dependent 21-bp siRNAs produced from CymRSV-derived dsRNA.

Of the 21- and 24-bp siRNA species, we studied only the former in this experiment, because AGO1-dependent RNAi generates a measurable silencing movement phenotype (that is, lack of *SUL* or *GFP*). Yet, there is no reason to exclude mobility of DCL3-dependent 24-nt siRNAs, which mediate locus-specific chromatin modifications upon loading into AGO4 (*12*). Using a micrografting procedure, we have obtained evidence that *Arabidopsis* endogenous siRNAs of all size classes are mobile from cell to cell and over long distances (*19*). Meanwhile, the experimental system described here now provides a handle to dissect the cell biology of siRNA movement in plants.

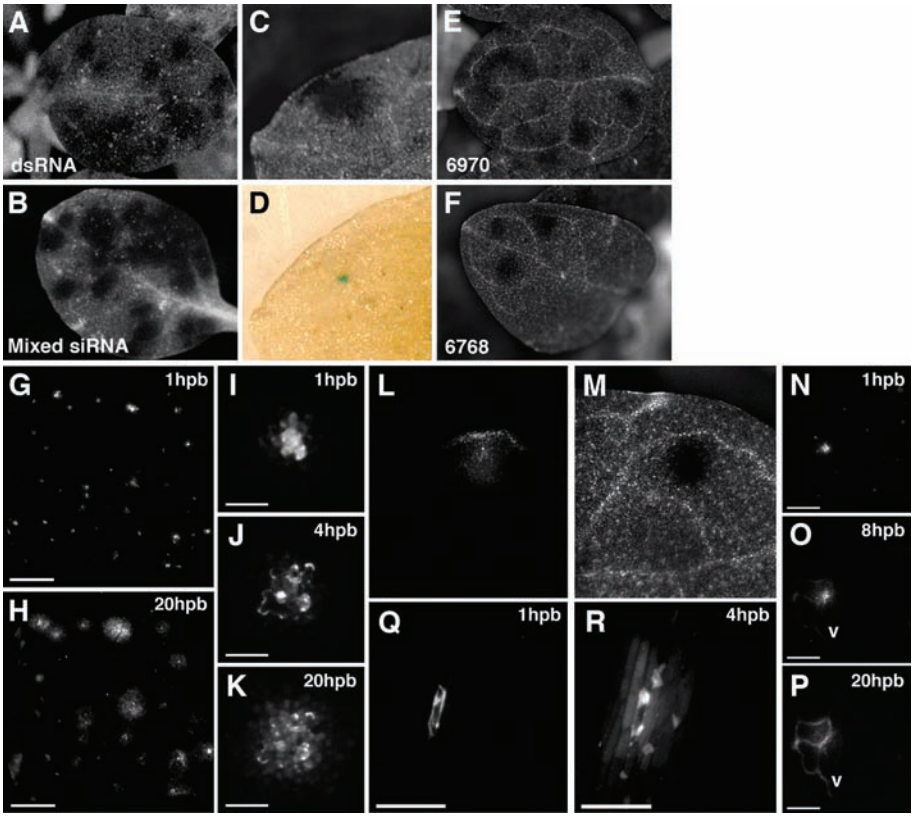

Fig. 4. Bombarded siRNAs trigger GFP silencing and move from cell to cell. (**A** and **B**) GFP-silencing foci on XD216 leaves triggered by *GFP*-derived dsRNA or a mix of three independent, chemically synthesized siRNAs duplexes. (**C** and **D**) An XD216 leaf cobombarded with GFP-targeting siRNA and GUS-expressing plasmid. GFP silencing is visible at 4 dpb (C). GUS staining was done at 4 dpb (D). (**E** and **F**) GFP-silencing foci on XD216 triggered by single GFP-targeting siRNA duplex 6768 or 6970. (**G** and **H**) *Arabidopsis* Col-0 leaf bombarded with ALEXA555-labeled siRNA 6768 at 1 hpb (G) and 20 hpb (H). (**I** to **K**) Same as in (G) and (H) at 1 hpb (I), 4 hpb (J), and 20 hpb (K) on turnip leaves. (**L** and **M**) Coincidence of ALEXA555-labeled siRNA 6768 (L) and GFP silencing (M) on XD216 at 4 dpb. (**N** and **P**) Bombarded Col-0 leaf at 1 hpb (N), 8 hpb (O), 20 hpb (P) showing that ALEXA555-labeled siRNA 6768 reaches the vascular system (v). (**Q** and **R**) Movement of ALEXA555-labeled siRNA 6768 within the vascular bundle at 1 hpb (Q) and 4 hpb (R). Scale bars: 500 μm for (G), (H), (N), (O), and (P); 100 μm for (I), (J), and (K); 200 μm for (Q) and (R).

References and Notes

1. D. Baulcombe, *Nature* **431**, 356 (2004).
2. O. Voinnet, *FEBS Lett.* **579**, 5858 (2005).
3. A. Deleris *et al.*, *Science* **313**, 68 (2006); published online 1 June 2006 (10.1126/science.1128214).
4. R. Schwab *et al.*, *PLoS ONE* **4**, e5980 (2009).
5. D. H. Chitwood *et al.*, *Genes Dev.* **23**, 549 (2009).
6. R. K. Slotkin *et al.*, *Cell* **136**, 461 (2009).
7. E. Allen, Z. Xie, A. M. Gustafson, J. C. Carrington, *Cell* **121**, 207 (2005).
8. P. Dunoyer, C. Himber, V. Ruiz-Ferrer, A. Alioua, O. Voinnet, *Nat. Genet.* **39**, 848 (2007).
9. P. Dunoyer, O. Voinnet, *Trends Plant Sci.* **14**, 643 (2009).
10. J. M. Vargason, G. Szittya, J. Burgyán, T. M. Hall, *Cell* **115**, 799 (2003).
11. Z. Mérai *et al.*, *J. Virol.* **80**, 5747 (2006).
12. T. A. Montgomery *et al.*, *Cell* **133**, 128 (2008).
13. H. Vaucheret, *Trends Plant Sci.* **13**, 350 (2008).

14. N. Baumberger, D. C. Baulcombe, *Proc. Natl. Acad. Sci. U.S.A.* **102**, 11928 (2005).
15. P. Brodersen *et al.*, *Science* **320**, 1185 (2008); published online 15 May 2008 (10.1126/science.1159151).
16. C. Himber, P. Dunoyer, G. Moissiard, C. Ritzenthaler, O. Voinnet, *EMBO J.* **22**, 4523 (2003).
17. S. Y. Berezhna, L. Supekova, F. Supek, P. G. Schultz, A. A. Deniz, *Proc. Natl. Acad. Sci. U.S.A.* **103**, 7682 (2006).
18. O. Voinnet, P. Vain, S. Angell, D. C. Baulcombe, *Cell* **95**, 177 (1998).
19. D. S. Schwarz *et al.*, *Cell* **115**, 199 (2003).
20. D. S. Schwarz, G. Hutvágner, B. Haley, P. D. Zamore, *Mol. Cell* **10**, 537 (2002).
21. Z. Havelda, C. Hornyik, A. Crescenzi, J. Burgyán, *J. Virol.* **77**, 6082 (2003).
22. P. Dunoyer *et al.*, *EMBO J.*, published online 22 April 2010 (10.1038/emboj.2010.65).
23. Research in O.V.'s laboratory is funded by a prize from the Bettencourt Foundation for Life Science Research and a starting grant from the European Research Council "Frontiers of RNAi" ERC 210890. P.D. and G.S. are supported by a research grant from Agence National pour la Recherche (ANR-08-JCJC-0063-01), J.C.C. is supported by grants from the NIH (AI43288) and the NSF (MCB-0618433), and A.T. is supported by a fellowship from the Japanese Society for the Promotion of Science. We thank J. Mutterrer for help with image acquisition, R. Wagner's team for plant care, and members of O.V.'s laboratory for critical reading of the manuscript.

Supporting Online Material

www.sciencemag.org/cgi/content/full/science.1185880/DC1
SOM Text
Figs. S1 to S5
References

14 December 2009; accepted 28 January 2010
Published online 22 April 2010;
10.1126/science.1185880
Include this information when citing this paper.

Genome-Wide Evolutionary Analysis of Eukaryotic DNA Methylation

Assaf Zemach, Ivy E. McDaniel, Pedro Silva, Daniel Zilberman*

Eukaryotic cytosine methylation represses transcription but also occurs in the bodies of active genes, and the extent of methylation biology conservation is unclear. We quantified DNA methylation in 17 eukaryotic genomes and found that gene body methylation is conserved between plants and animals, whereas selective methylation of transposons is not. We show that methylation of plant transposons in the CHG context extends to green algae and that exclusion of histone H2A.Z from methylated DNA is conserved between plants and animals, and we present evidence for RNA-directed DNA methylation of fungal genes. Our data demonstrate that extant DNA methylation systems are mosaics of conserved and derived features, and indicate that gene body methylation is an ancient property of eukaryotic genomes.

Our knowledge about cytosine methylation has been derived mainly from four species: humans, mouse, *Arabidopsis thaliana*, and *Neurospora crassa* (*1*). Transposons and repeats are virtually uniformly methylated in all four, which suggests that transposon defense is an ancient function of methylation (*1*, *2*). The expression of imprinted genes is regulated by DNA methylation in *A. thaliana* and mammals (*3*), and in both cases the bodies of active genes are methylated (*4*–*6*). However, these analogies do not necessarily imply conservation. Regulation of imprinting has evolved independently in mammals and flowering plants (*3*). Many transposons are not methylated in the tunicate *Ciona intestinalis* (*7*), and the transposon-rich silk moth (*Bombyx mori*) genome contains low levels of 5-methylcytosine (*8*), putting into question the conservation of transposon methylation (*9*). To understand how eukaryotic DNA methylation has evolved, we quantified DNA methylation by deep bisulfite sequencing in the genomes of five plants, seven animals, and five fungi (figs. S1 to S6 and tables S1 to S3). We also profiled transcription in these species by deep sequencing of cDNA (*10*). The results reveal a complex evolutionary history of the DNA methylation pathway and allow us to reconstruct a plausible ancestral state.

Rice (*Oryza sativa*) is a model monocot that contains Dnmt1 (CG methyltransferase), Dnmt3 [de novo methyltransferase responsible for plant CHH methylation (H = A, C, or T)], and CMT (plant-specific CHG methyltransferase) orthologs (*1*) (figs. S1 to S5 and table S4). Our data show that CG methylation is lowest from 100 base pairs (bp) upstream of the transcriptional start site (TSS) of rice genes to 500 bp within the transcript, plateauing around 1.5 kb after the TSS (Fig. 1A). Non-CG methylation is essentially absent from genes, whereas methylation in all contexts is abundant in transposable elements (TEs; Fig. 1, A and B), with short TEs particularly enriched in CHH methylation (fig. S7). Consistent with functioning to repress transcription, gene expression varies inversely with methylation of the TSS-proximal region (Fig. 1C). The same pattern is present at the 3′ end of genes, which suggests that lack of methylation around the transcription termination site is also important for gene expression (Fig. 1C). Within the gene body plateau, rice methylation exhibits a parabolic relationship with transcription: Modestly expressed genes are most likely to be methylated, whereas genes at either transcriptional extreme are least likely to be methylated (Fig. 1C and fig. S8). In all salient features, rice methylation patterns closely resemble those of *A. thaliana* (*5*, *6*).

We examined methylation in two early-diverging land plants: *Selaginella moellendorffii* and *Physcomitrella patens* (fig. S1) (*11*), both possessing Dnmt1, Dnmt3, and CMT orthologs (figs. S1 to S5). *S. moellendorffii* TEs are methylated in the CG, CHG, and CHH contexts, but unlike the angiosperms, genes have little methylation, and there is essentially no methylation around the TSS regardless of transcription (Fig. 1, D to F, and table S1). *P. patens* methylation patterns closely resemble those of *S. moellendorffii* (table S1 and fig. S9) (*10*). DNA methylation in these plants is strictly segregated away from genes.

We analyzed two green algae, *Chlorella* sp. NC64A and *Volvox carteri* (figs. S1 to S3). *Chlorella* has the greatest amount of CG methylation of any organism analyzed here (Fig. 1, G to I, and table S1): Genes are methylated virtually without exception (fig. S10), with a sharp drop of methylation at the promoter (Fig. 1G). Promoter methylation correlates negatively with gene expression (Fig. 1I), which suggests that TSS-proximal methylation represses transcription, as it does in land plants. Although CMT genes have thus far been described only in land plants (*1*), *Chlorella* contains a CMT homolog (figs. S1 to S3) and a substantial amount of CHG methylation (table S1), which is concentrated in repetitive elements and excluded from genes (Fig. 1, G to I). The *V. carteri* genome is much less methylated exclusively in the CG context, with a similar relationship between promoter methylation and transcription, and displays preferential methylation of TEs (table S1 and fig. S9). Methylation of both gene bodies and TEs thus appears to be an ancient property of plants.

The genome of the puffer fish *Tetraodon nigroviridis* is virtually devoid of transposable elements (*12*), yet we find heavy methylation exclusively at CG sites, the vast majority of which is found in genes, although TEs do show particularly dense methylation (Fig. 2, A and B, and table S1). Genes exhibit a prominent dip in methylation just upstream of the TSS, and reduced promoter methylation correlates with enhanced expression (Fig. 2A). Gene body methylation exhibits the same relationship with transcription that exists in *A. thaliana* and rice—a roughly parabolic curve with the most methylated genes around the 70th transcription percentile (fig. S8).

The similarities between plants and vertebrates prompted us to ask whether aspects of the

Department of Plant and Microbial Biology, 211 Koshland Hall, University of California, Berkeley, CA 94720, USA.

*To whom correspondence should be addressed. E-mail: danielz@berkeley.edu

ERRATUM

Post date 15 April 2011

Reports: "Small RNA duplexes function as mobile silencing signals between plant cells" by P. Dunoyer *et al.* (14 May 2010, p. 912). The image in Fig. 3B (center panel) was previously published as Fig. 1e in P. Dunoyer *et al., Nat. Genet.* **39**, 848 (2007).